JINR University Centre **INTEREST**

Wave 11

Project: "Radiation Protection and the Safety of Radiation Sources"

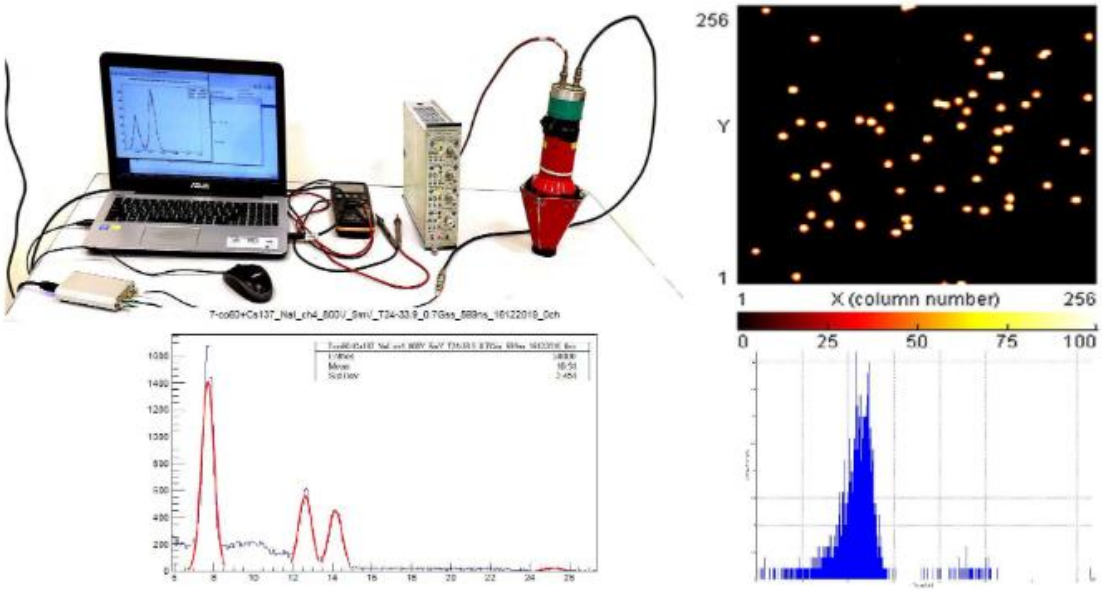

SUPERVISOR:

Dr Said AbouElazm

Dzhelepov Laboratory of Nuclear Problems

said42@hotmail.com

PROJECT PARTICIPANT:

B.Sc. Kissy Dayana Iznaga Pino

Higher Institute of Technologies and Applied Sciences, University of Havana

dayznagap00@gmail.com

Determination of the relationship between the applied voltage and the resolution of a BGO detector using a Co^{60} radioactive source.

Kissy Dayana Iznaga Pino

1. Introduction

Bismuth germanate (BGO) detectors are widely used in various applications due to their high efficiency and stopping power for gamma ray detection. Several studies confirm the versatility and effectiveness of these detectors for medical and nuclear physics applications. In positron emission tomography (PET), BGO detectors coupled to photodiodes have shown promise in improving spatial resolution (Derenzo, 1984). BGO active shields are also used to improve the sensitivity of high-purity germanium detectors by suppressing background radiation (Kosir et al., 2024). Monte Carlo simulations have been used to compare the response functions of BGO and NaI(Tl) detectors, highlighting the superior efficiency of BGO but its lower resolution (Orion and Wielopolski, 2000).

Understanding the relationship between detector resolution and applied voltage is essential for particle detection and imaging. For this reason, the purpose of this work is to determine the relationship between the energy resolution and the voltage applied to a BGO detector.

2. Experiment

The responses of a BGO detector are analyzed, using a Co^{60} radioactive source and varying the applied voltage from 1200V to 2000V.

To determine the energy resolution of the detector, the definition of resolution was used:

$$R = \frac{FWHM}{H_o}$$

where FWHM (*Full Width at Half Maximum*), is the width of the distribution measured at the average height of the peak, and H_o, its centroid. This magnitude is dimensionless and is usually expressed as a percentage.

The FWHM value was determined as

$$FWHM = 2.35 * \sigma$$

where σ is the standard deviation of the distribution.

The H_o and σ values were obtained by using the ROOT software.

3. Results and discussion

Table 1 shows the resolution values obtained for the BGO detector at 1173 keV, making variations in the applied voltage. The peaks were located by their maximum and not according to the position of their centroid.

Table 1 Energy resolution for the 1173 keV peak of Co^{60} and different voltages.

Sample	σ	H_o	Resolution (%)
12	0,366575	1,65575	52,02785747
13	0,222535	1,34099	38,9978486
14	0,264922	1,92132	32,40307185
15	0,397371	2,99922	31,13549023
16	0,536877	4,42007	28,54391333
17	0,741146	6,11454	28,48445018
19	1,23591	10,7016	27,13975948
20	1,54388	13,6882	26,50544264

As can be seen in Table 1, the energy resolution obtained for the detector in question ranges from 26-52% at 1173 keV. Compared to other detectors, BGO detectors tend to have worse energy resolution due to statistical fluctuations in photon production. In research, energy resolution values for BGO detectors have been reported in the range of 10-20% at 662 keV. However, some studies have shown that resolution can vary depending on factors such as crystal quality, detector configuration, and operating conditions. However, in preclinical PET scanners, BGO detectors have demonstrated adequate performance characteristics, including energy resolution ranging from 15.5% to 42.7% FWHM (Zhang et al., 2010).

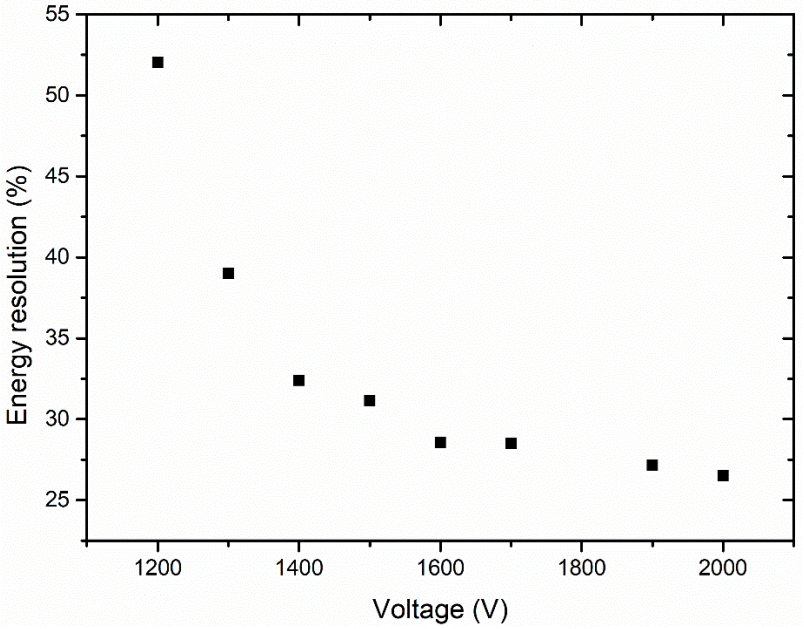

Figure 1 Variation of detector energy resolution with voltage.

The lower the resolution of a detector, the greater its ability to distinguish two radiations of very close energies. In this case, the energy resolution of the detector improves as the voltage is increased. As can be seen in Figure 1, above

1600 V the energy resolution improves by around 27.67%, approaching the upper limit reported in the literature. However, great care must be taken with increasing the voltage as it may damage the detector.

4. Conclusions

In the present work, the relationship between the energy resolution of a BGO detector and the applied voltage was analyzed, using a Co^{60} source and making voltage variations in a range of 1200-2000 V. Finally, it was determined that, for voltage values Above 1600 V, the energy resolution of the detector improves by around 27.67% at 1173 keV.

Referencias:

S. Derenzo. ***Initial Characterization of a Bgo-Photodiode Detector for High Resolution Positron Emission Tomography***. IEEE Transactions on Nuclear Science, 1984.

G. Kosir, J. Vesic, I. Kojouharov, H. Schaffner, J. Gerl, N. Kurz, M. Reese, M. Vencelj. ***BGO active shield for DEGAS***. Nuclear Instruments and Methods in Physics Research Section A: Accelerators, Spectrometers, Detectors and Associated Equipment, 2024.

I. Orion, L. Wielopolski. ***Response Function of the BGO and NaI(Tl) Detectors Using Monte Carlo Simulations***. Annals of the New York Academy of Sciences, 2000.

H. Zhang, N. Vu, Q. Bao, R. Silverman, B. Berry-Pusey, A. Douraghy, D. Williams, F.R. Rannou, D. Stout, A. Chatziioannou. ***Performance Characteristics of BGO Detectors for a Low Cost Preclinical PET Scanner***. IEEE Transactions on Nuclear Science, 2010.

N.W. Brzostowicz. ***Caracterización de un detector de centelleo de última generación de $LaCl_3(Ce)$***. Estancias en centros de investigación asociados al CSIC.

Determination of the relationship between the applied voltage and the resolution of a NaI detector using a Co^{60} radioactive source.

Kissy Dayana Iznaga Pino

1. Introduction

Sodium iodide (NaI) detectors are widely used for gamma-ray detection due to their high efficiency and good energy resolution. Large NaI detectors can achieve excellent energy resolution, with one system demonstrating 1.6% resolution at 22.6 MeV (Håkansson et al., 1988). NaI detectors are also suitable for in-situ measurements of 137Cs in alpine environments (Schaub et al., 2010). Recent developments include CMOS-coupled NaI scintillation detectors, which offer excellent linearity over a wide range of activity levels without requiring dead-time correction. These detectors demonstrate similar sensitivity and noise characteristics to photomultiplier tube-based systems on short time scales (Bergeson et al., 2020).

Understanding the relationship between detector resolution and applied voltage is essential for particle detection and imaging. For this reason, the purpose of this work is to determine the relationship between the energy resolution and the voltage applied to a NaI detector.

2. Experiment

The responses of a NaI detector are analyzed, using a Co^{60} radioactive source and varying the applied voltage from 900V to 1300V.

To determine the energy resolution of the detector, the definition of resolution was used:

$$R = \frac{FWHM}{H_o}$$

where FWHM (*Full Width at Half Maximum*), is the width of the distribution measured at the average height of the peak, and H_o, its centroid. This magnitude is dimensionless and is usually expressed as a percentage.

The FWHM value was determined as

$$FWHM = 2.35 * \sigma$$

where σ is the standard deviation of the distribution.

The H_o and σ values were obtained by using the ROOT software.

3. Results and discussion

Table 1 shows the resolution values obtained for the NaI detector at 1173 keV, making variations in the applied voltage. The peaks were located by their maximum and not according to the position of their centroid.

Table 1 Energy resolution for the 1173 keV peak of Co^{60} and different voltages.

Sample	σ	H_o	Resolution (%)
2	0,562653	23,699700	5,579119
3	0,920517	40,681700	5,317415
4	1,486350	65,829300	5,306030
5	2,009000	98,789300	4,779009
6	2,466190	137,393000	4,218225

As can be seen in Table 1, the energy resolution obtained for the detector in question ranges from 4-6% at 1173 keV. The scintillation detectors used in gamma ray spectroscopy usually have energy resolutions in the range of 5-10%, so one could conclude that our NaI detector has good energy resolution. Sharma et al. (2023) found that resolution improved with increasing gamma-ray energy, ranging from 11.27% at 356 keV to 4.74% at 1330 keV.

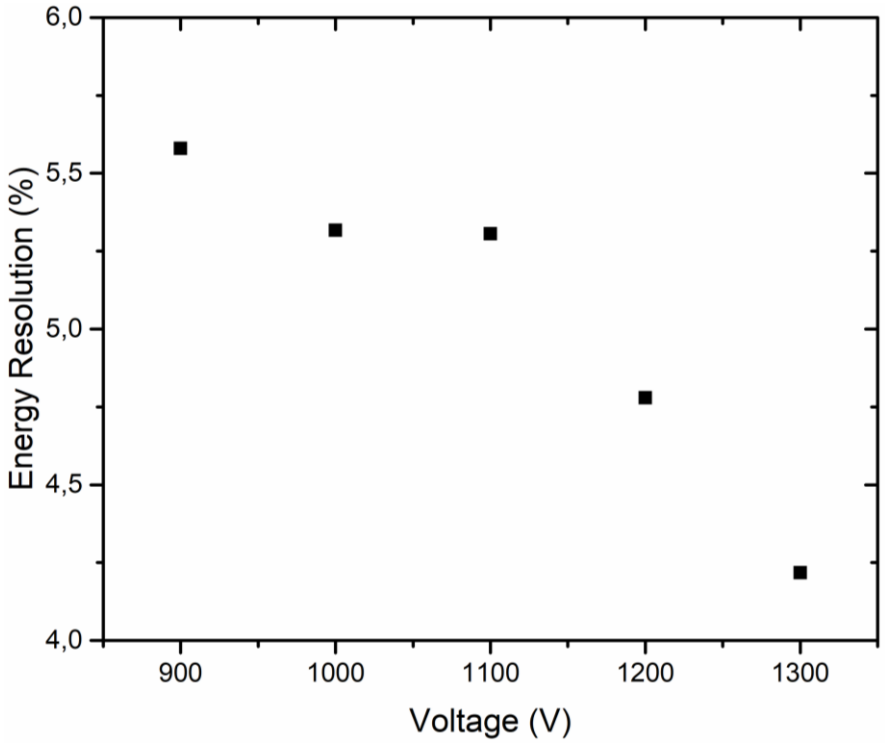

Figure 1 Variation of detector energy resolution with voltage.

The lower the resolution of a detector, the greater its ability to distinguish two radiations of very close energies. In this case, the energy resolution of the detector improves as the voltage is increased. As can be seen in Figure 1, above 1100 V the energy resolution improves to below 5%. However, great care must be taken with increasing the voltage as it may damage the detector. It is noticeable that NaI detectors have better energy resolution than BGO detectors.

4. Conclusions

In the present work, the relationship between the energy resolution of a NaI detector and the applied voltage was analyzed, using a Co^{60} source and making voltage variations in a range of 900-1300 V. Good resolution values were obtained that improved with the increase in voltage, these being less than 5% at 1173 keV for voltages greater than 1100V.

Reference:

A. Håkansson, J. Blomgren, S. Crona, A. Likar, A. Lindholm, L. Nilsson, N. Olsson, R. Zorro. ***A large high-resolution sodium iodide spectrometer***. Nuclear Instruments and Methods in Physics Research Section A: Accelerators, Spectrometers, Detectors and Associated Equipment, Volume 273, Issue 1, 1 December 1988, Pages 211-217.

M. Schaub, N. Konz, K. Meusburger, C. Alewell. ***Application of in-situ measurement to determine 137Cs in the Swiss Alps***. Journal of Environmental Radioactivity, 2010.

S. Bergeson, M. Ware, Jeremy Hawk. ***CMOS-coupled NaI scintillation detector for gamma decay measurements***. Review of Scientific Instruments, 2020.

Jibon Sharma, A. Patowary, Nara M. Singh. ***Determination of full energy peak efficiency and resolution of NaI(Tl) detector using Gamma-Ray Spectroscopy***. The Proceedings of the International Conference on Nuclear Engineering (ICONE), 2023.

N.W. Brzostowicz. ***Caracterización de un detector de centelleo de última generación de $LaCl_3(Ce)$***. Estancias en centros de investigación asociados al CSIC.

Energy calibration of BGO and NaI detectors.

Kissy Dayana Iznaga Pino

1. Introduction

Since there is a relationship between the size of the impulse produced by an incident particle and its energy, it is possible in certain cases to obtain a function that relates the channel numbers to the energies attributed to them. This process is called energy calibration, which in most cases corresponds to a linear function. To do this, it is necessary to have certified radioactive sources with known energies.

To obtain the calibration equation you must have several pairs of data: energy - channel number. If the relationship is linear, the calibration curve is expressed as:

$$E = mCh + n \tag{1}$$

where *E* represents the energy expressed in its corresponding unit of measurement, *m* is the slope of the line, *Ch* represents the channel number and *n* is the intercept of the line on the ordinate axis. These factors do not depend on the radioactive sample or the detector used, but rather depend on the electronic pulse amplification and classification devices, the power supply of the photomultiplier, the characteristics of the detector, among others.

The objective of this work is to perform the energy calibration of BGO and NaI detectors with known radioactive sources.

2. Experiment

To obtain the calibration curve of the BGO and NaI detectors, the radioactive sources Cs^{137} and Co^{60} were used, which are gamma emitters of known energies. ROOT software was used for data treatment and analysis.

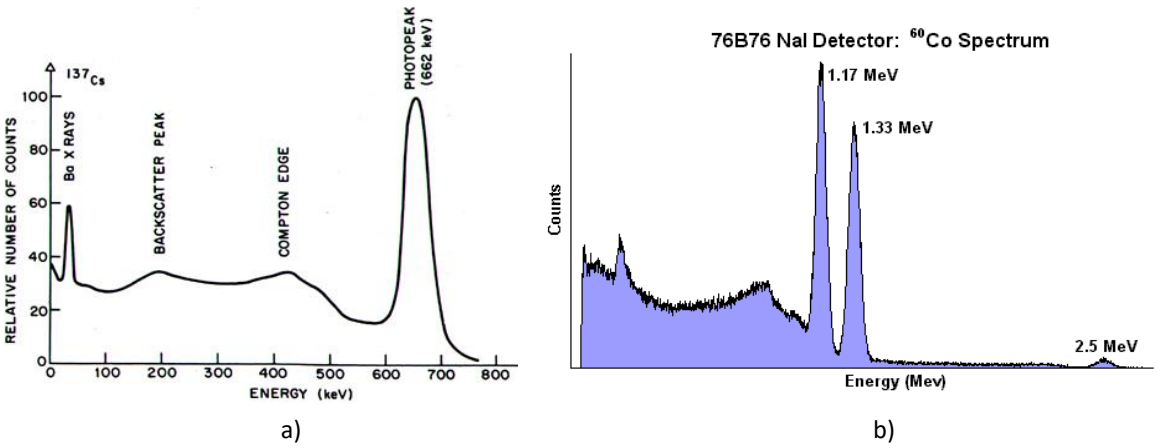

Figure 1 a) Cs^{137} Gamma spectrum, b) Co^{60} Gamma spectrum

3. Results and discussion

BGO Detector Calibration

With the help of the ROOT software, the peaks were selected and fitted to a Gaussian distribution, to subsequently determine its centroid. With the centroids determined and the known energies of each peak, a linear regression was performed that resulted in the following calibration line:

$$E\ (keV) = 102.72734 * Ch - 4.94908 \quad (2)$$

Table 1 Data used for BGO detector calibration.

Source	Channel	Energy (keV)
Cs^{137}	6,47458	662
Co^{60}	12,2719	1253
Co^{60}	24,3759	2500

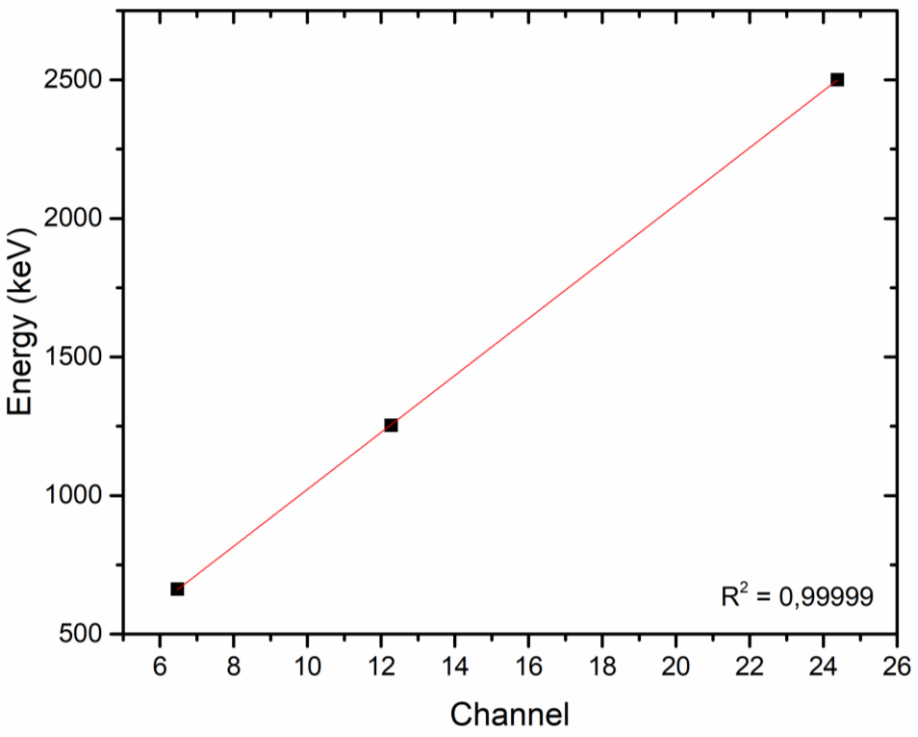

Figure 2 Linear fit performed to obtain the linear calibration equation: $E\ (keV) = 102.72734 * Ch - 4.94908$, where E is the energy in keV and Ch is the channel number.

NaI Detector Calibration

With the help of the ROOT software, the peaks were selected and fitted to a Gaussian distribution, to subsequently determine its centroid. With the centroids determined and the known energies of each peak, a linear regression was performed that resulted in the following calibration line:

$$E\ (keV) = 105.23113 * Ch - 153.00768 \quad (3)$$

Table 2 Data used for NaI detector calibration.

Source	Channel	Energy (keV)
Cs^{137}	7,70305	662
Co^{60}	12,6323	1173
Co^{60}	14,152	1333
Co^{60}	25,1911	2500

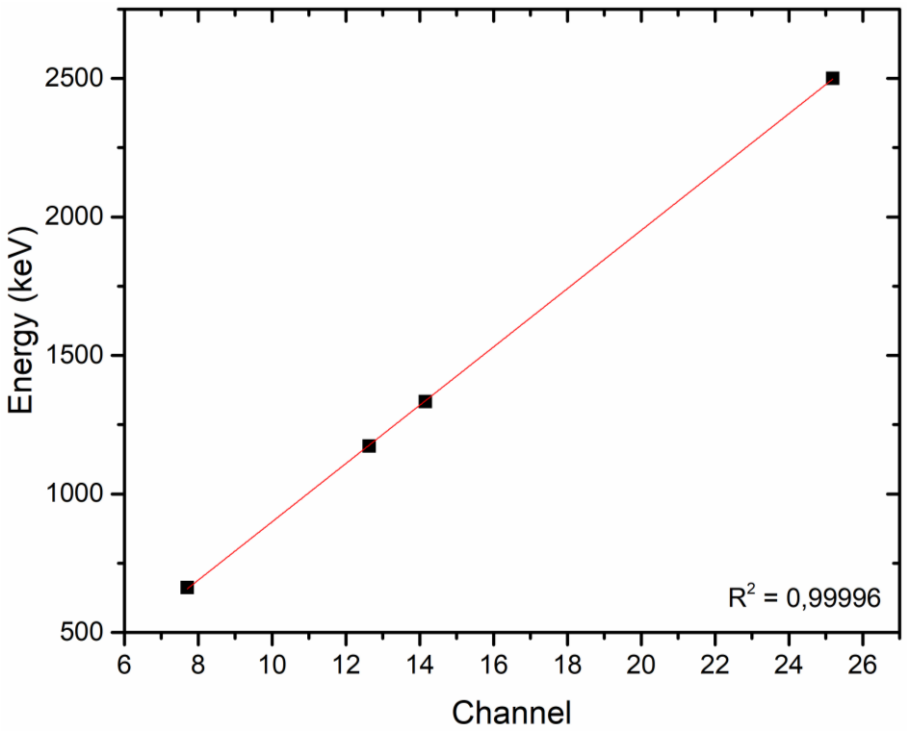

Figure 3 Linear fit performed to obtain the linear calibration equation: $E\ (keV) = 105.23113 * Ch - 153.00768$, where E is the energy in keV and Ch is the channel number.

4. Conclusions

The energy calibration of the BGO and NaI detectors was carried out using radiation sources of known energies Co^{60} and Cs^{137}. For the BGO detector, the calibration equation was obtained: $E\ (keV) = 102.72734 * Ch - 4.94908$, where *E* is the energy in KeV and *Ch* is the channel number corresponding to the peak centroid. For the NaI detector, the calibration equation was obtained: $E\ (keV) = 105.23113 * Ch - 153.00768$.

Reference

N. W. Brzostowicz. ***Caracterización de un detector de centelleo de última generación de $LaCl_3$(Ce)***. Estancias en centros de investigación asociados al CSIC.

Calibration and determination of the resolution of the X-123CdTe detector.

Kissy Dayana Iznaga Pino

1. Introduction

Cadmium telluride (CdTe) semiconductor detectors have gained significant attention for X-ray and gamma-ray detection due to their high atomic numbers and large bandgap energies, allowing operation at room temperature (Takahashi and Watanabe, 2001). These detectors offer improved spatial and energetic resolution compared to traditional scintillation detectors, making them suitable for various medical imaging applications, including single-photon emission computed tomography (Abbaspour et al., 2017). Despite their advantages, CdTe detectors face challenges related to charge loss due to low hole mobility and short lifetime (Takahashi and Watanabe, 2001). Recent advances in crystal production and electrode design have improved spectral properties and overall detector performance (Sordo et al., 2009). These advances have expanded the potential applications of these detectors in the astrophysical and medical fields, and ongoing research is focused on further improving their capabilities (Sordo et al., 2009).

In this report, the resolution of the X-123CdTe detector will be determined, as well as its energy calibration.

2. Experiment

2.1 Energy resolution calculation

To determine the resolution of the X-123CdTe detector, its response to a Co^{57} radioactive source was analyzed using the Amptek_DppMCA software. To carry out the calculation, the definition of resolution was used:

$$R = \frac{FWHM}{H_o}$$

where FWHM (Full Width at Half Maximum), is the width of the distribution measured at the average height of the peak, and H_o, its centroid. This magnitude is dimensionless and is usually expressed as a percentage. The H_o and FWHM values were obtained using the aforementioned software.

2.2 Energy calibration

To perform the energy calibration, the radioactive sources Cs^{137}, Co^{60} and Am^{241} were used, which are gamma emitters of known energies. For data treatment and analysis, the Amptek_DppMCA software was used in the same way, with the help of the OriginPro9 software to construct the calibration curve.

3. Results and discussion

3.1 Energy resolution calculation

Table 1 shows the FWHM and centroid data obtained for the Co^{57} spectrum, as well as the respective resolution value determined using these values. The peaks were located by their maximum and not according to the position of their centroid.

Table 1 Parameters and energy resolution for the 122 keV peak of Co^{57}.

$FWHM$	H_o	Resolution (%)
4,1042	322,57	1.27

As can be seen in Table 1, the resolution obtained for the X-123CdTe detector is 1.27% at 122 keV, which represents a good resolution, since the characteristic resolutions of semiconductor detectors are around 1% and even less.

3.2 Energy calibration

With the help of the Amptek_DppMCA software, the peaks were selected and fitted to an ROI to subsequently determine its centroid. With the centroids determined and the known energies of each peak, a linear regression was performed in the OriginPro9 software that resulted in the following calibration line:

$$E\ (keV) = 1.70369 * Ch - 452.07993$$

Table 2 Data used for calibration of the X-123CdTe detector

Source	Channel	Energy (keV)
Cs^{137}	654.27	662
Co^{57}	322.57	122
Am^{241}	314.32	59.5

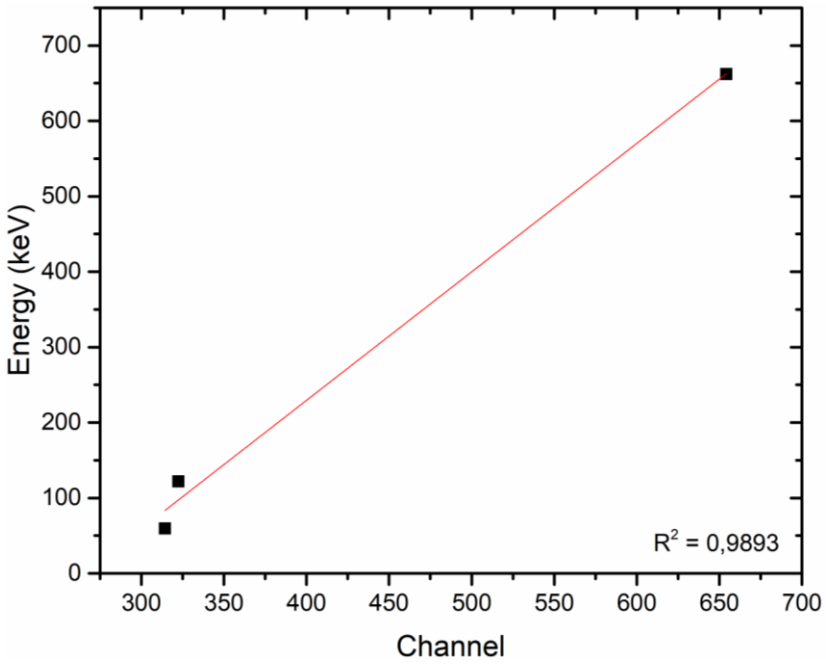

Figure 1 Linear fit performed to obtain the linear calibration equation: $E\ (keV) = 1.70369 * Ch - 452.07993$, where E is the energy in keV and Ch is the channel number.

4. Conclusions

In this report, the resolution of the X-123CdTe detector was determined using a Co^{57} source, which turned out to be 1.27% at 122 keV. The calibration curve for said detector was also carried out with the known sources Cs^{137}, Co^{57} and Am^{241}, which turned out to be $E\ (keV) = 1.70369 * Ch - 452.07993$, where E is the energy in keV and Ch is the channel number.

Reference

Tadayui Takahashi, S. Watanabe. ***Recent progress in CdTe and CdZnTe detectors***. IEEE Transactions on Nuclear Science, Vol. 48, No. 4 (2001).

S. Abbaspour, B. Mahmoudian, J. Islamian. ***Cadmium Telluride Semiconductor Detector for Improved Spatial and Energy Resolution Radioisotopic Imaging***. World Journal of Nuclear Medicine (2017).

S. Sordo, L. Abbene, E. Caroli, A. Mancini, A. Zappettini, P. Ubertini. ***Progress in the Development of CdTe and CdZnTe Semiconductor Radiation Detectors for Astrophysical and Medical Applications***. Italian National Conference on Sensors (2009).

Determination of the attenuation coefficient of Al and Cu using the X-123CdTe detector.

Kissy Dayana Iznaga Pino

1. Introduction

The attenuation of ionizing radiation in medical physics is a crucial topic for radiation protection and imaging. Computational simulations can model radiation attenuation through various materials, providing insights into shielding requirements and dose calculations (Silva, 2012; Páez López et al., 2022). The interaction of X-rays with matter involves processes such as coherent scattering, photoelectric effect, Compton scattering, pair production, and photodisintegration, which contribute to beam attenuation depending on photon energy and medium composition (Sethi, 2006).

The objective of this work is to determine the attenuation coefficient of Al and Cu, which are materials used in shielding certain radioactive sources.

2. Experiment

The X-123CdTe detector and a radioactive source of Am^{241} are used. To determine the attenuation coefficient of Al and Cu, the expression was used:

$$I = I_0 e^{-\mu x} \tag{1}$$

where I_o is the initial intensity of the radiation beam, I is the intensity of the radiation beam once it passes through the material, μ is the attenuation coefficient of the material and x is the thickness of the material.

The values referring to the intensities of the beams were obtained using the DppMCA software. For this, the areas under the photoabsorption peaks were analyzed, since the emission energy of Am^{241} is 59.5 keV and it is observed that the total attenuation of the photon is through photoelectric absorption (figure 1).

Working mathematically with expression 1, we can arrive at the following relationship that corresponds to a linear fit, where the slope of the fit will be the attenuation coefficient of the material:

$$\ln \frac{I_o}{I} = \mu * x \tag{2}$$

3. Results and discussion

Table 1 shows the beam intensity values before and after passing through the Al, as well as its thickness.

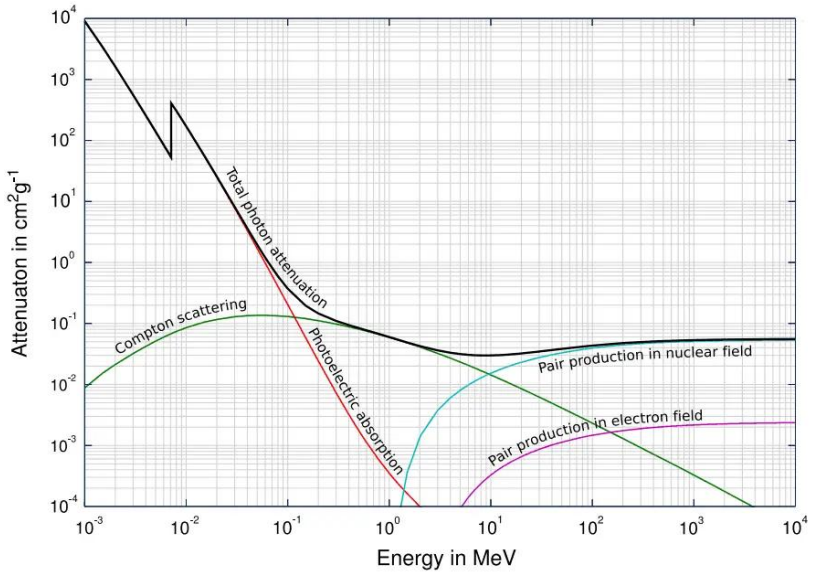

Figure 1 *Total photon cross sections.*

Table 1 *Values used to determine the linear attenuation coefficient of Al.*

X (cm)	Io	I	Io/I	Ln (Io/I)
0,052	2849	2778	1,025558	0,025237
0,11	2849	2471	1,152975	0,142345
0,16	2849	2457	1,159544	0,148027
0,22	2849	2387	1,193548	0,176931
0,281	2849	2363	1,205671	0,187036
0,3	2849	2134	1,335052	0,28897
0,5	2849	1896	1,502637	0,407222
0,8	2849	1386	2,055556	0,720546
1,6	2849	741	3,844804	1,346723
2,897	2849	277	10,2852	2,330706
3,397	2849	213	13,37559	2,593431
4,374	2849	86	33,12791	3,500376

After performing the linear fit (Figure 2), it was obtained that the linear attenuation coefficient of Al is $0.7866\ cm^{-1}$ for 59.5 keV (≈ 6*10^{-2} MeV) of energy. Since the density of aluminum is 2.7 g/cm^3, the mass attenuation coefficient was determined, this being $\mu\ /\ \rho = 0.2913\ cm^2\ /\ g$. Table 2 shows the tabulated mass attenuation coefficient value for Al as a function of the incident photon energy. For an energy of 6*10^{-2} MeV, the mass attenuation coefficient of Al is $\mu\ /\ \rho = 0.2778\ cm^2\ /\ g$. Therefore, the result reported in this work has a relative error of 4.86%.

Table 3 shows the intensity values of the beam before and after passing through the Cu, as well as its thickness.

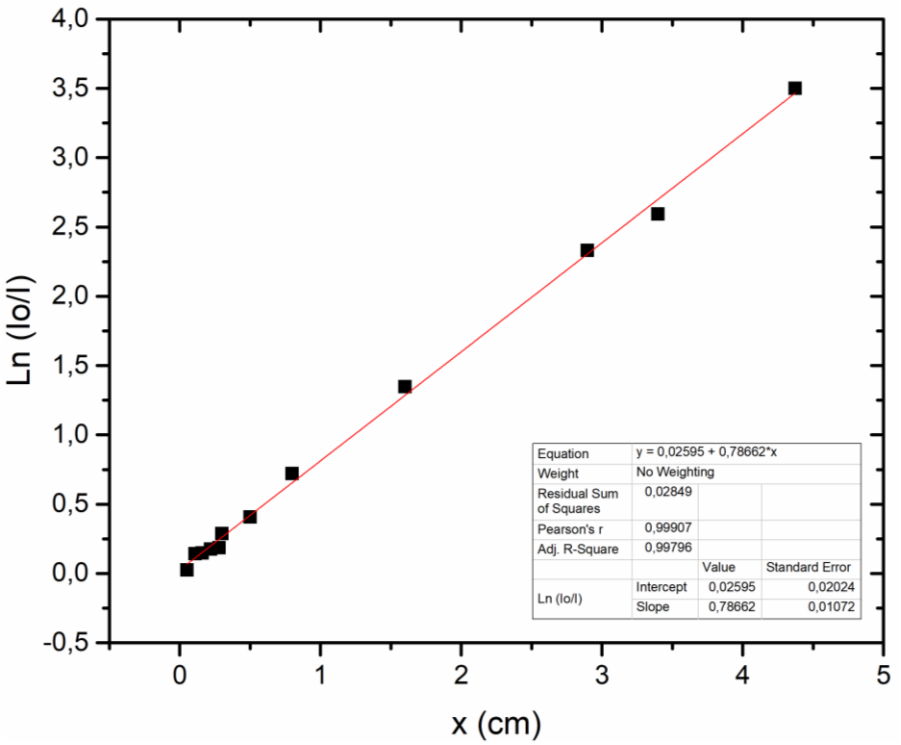

Figure 2 *Linear attenuation curve for Al.*

Table 2 *Values of mass attenuation coefficients of Cu and Al as a function of photon energy.*

Copper
$Z = 29$

ASCII format

	Energy (MeV)	μ/ρ (cm^2/g)	μ_{en}/ρ (cm^2/g)
	1.00000E-03	1.057E+04	1.049E+04
	1.04695E-03	9.307E+03	9.241E+03
	1.09610E-03	8.242E+03	8.186E+03
L1	1.09610E-03	9.347E+03	9.282E+03
	1.50000E-03	4.418E+03	4.393E+03
	2.00000E-03	2.154E+03	2.142E+03
	3.00000E-03	7.488E+02	7.430E+02
	4.00000E-03	3.473E+02	3.432E+02
	5.00000E-03	1.899E+02	1.866E+02
	6.00000E-03	1.156E+02	1.128E+02
	8.00000E-03	5.255E+01	5.054E+01
	8.97890E-03	3.829E+01	3.652E+01
K	8.97890E-03	2.784E+02	1.824E+02
	1.00000E-02	2.159E+02	1.484E+02
	1.50000E-02	7.405E+01	5.788E+01
	2.00000E-02	3.379E+01	2.788E+01
	3.00000E-02	1.092E+01	9.349E+00
	4.00000E-02	4.862E+00	4.163E+00
	5.00000E-02	2.613E+00	2.192E+00
	6.00000E-02	1.593E+00	1.290E+00
	8.00000E-02	7.630E-01	5.581E-01
	1.00000E-01	4.584E-01	2.949E-01
	1.50000E-01	2.217E-01	1.027E-01
	2.00000E-01	1.559E-01	5.781E-02
	3.00000E-01	1.119E-01	3.617E-02
	4.00000E-01	9.413E-02	3.121E-02
	5.00000E-01	8.362E-02	2.933E-02
	6.00000E-01	7.625E-02	2.826E-02
	8.00000E-01	6.605E-02	2.681E-02
	1.00000E+00	5.901E-02	2.562E-02
	1.25000E+00	5.261E-02	2.428E-02
	1.50000E+00	4.803E-02	2.316E-02
	2.00000E+00	4.205E-02	2.160E-02
	3.00000E+00	3.599E-02	2.023E-02
	4.00000E+00	3.318E-02	1.989E-02
	5.00000E+00	3.177E-02	1.998E-02
	6.00000E+00	3.108E-02	2.027E-02
	8.00000E+00	3.074E-02	2.100E-02
	1.00000E+01	3.103E-02	2.174E-02
	1.50000E+01	3.247E-02	2.309E-02
	2.00000E+01	3.408E-02	2.387E-02

Aluminum
$Z = 13$

ASCII format

	Energy (MeV)	μ/ρ (cm^2/g)	μ_{en}/ρ (cm^2/g)
	1.00000E-03	1.185E+03	1.183E+03
	1.50000E-03	4.022E+02	4.001E+02
	1.55960E-03	3.621E+02	3.600E+02
K	1.55960E-03	3.957E+03	3.829E+03
	2.00000E-03	2.263E+03	2.204E+03
	3.00000E-03	7.880E+02	7.732E+02
	4.00000E-03	3.605E+02	3.545E+02
	5.00000E-03	1.934E+02	1.902E+02
	6.00000E-03	1.153E+02	1.133E+02
	8.00000E-03	5.033E+01	4.918E+01
	1.00000E-02	2.623E+01	2.543E+01
	1.50000E-02	7.955E+00	7.487E+00
	2.00000E-02	3.441E+00	3.094E+00
	3.00000E-02	1.128E+00	8.778E-01
	4.00000E-02	5.685E-01	3.601E-01
	5.00000E-02	3.681E-01	1.840E-01
	6.00000E-02	2.778E-01	1.099E-01
	8.00000E-02	2.018E-01	5.511E-02
	1.00000E-01	1.704E-01	3.794E-02
	1.50000E-01	1.378E-01	2.827E-02
	2.00000E-01	1.223E-01	2.745E-02
	3.00000E-01	1.042E-01	2.816E-02
	4.00000E-01	9.276E-02	2.862E-02
	5.00000E-01	8.445E-02	2.868E-02
	6.00000E-01	7.802E-02	2.851E-02
	8.00000E-01	6.841E-02	2.778E-02
	1.00000E+00	6.146E-02	2.686E-02
	1.25000E+00	5.496E-02	2.565E-02
	1.50000E+00	5.006E-02	2.451E-02
	2.00000E+00	4.324E-02	2.266E-02
	3.00000E+00	3.541E-02	2.024E-02
	4.00000E+00	3.106E-02	1.882E-02
	5.00000E+00	2.836E-02	1.795E-02
	6.00000E+00	2.655E-02	1.739E-02
	8.00000E+00	2.437E-02	1.678E-02
	1.00000E+01	2.318E-02	1.650E-02
	1.50000E+01	2.195E-02	1.631E-02
	2.00000E+01	2.168E-02	1.633E-02

Table 3. *Values used to determine the linear attenuation coefficient of Cu.*

X (cm)	Io	I	Io/I	Ln (Io/I)
0,02	2634	2085	1,26330935	0,23373475
0,05	2634	1490	1,76778523	0,56972748
0,07	2634	1215	2,16790123	0,77375953
0,1	2634	701	3,7574893	1,323751
0,15	2634	298	8,83892617	2,1791654
0,2	2634	160	16,4625	2,80108507
0,25	2634	73	36,0821918	3,58579944

After performing the linear fit (Figure 3), it was obtained that the linear attenuation coefficient of Cu is $14.93\ cm^{-1}$ for 59.5 keV (≈ 6*10^{-2} MeV) of energy. Since the density of copper is 8.96 g/cm^3, the mass attenuation coefficient was determined, this being $\mu / \rho = 1.666\ cm^2 / g$. Table 2 shows the tabulated mass attenuation coefficient value for Cu as a function of the incident photon energy. For an energy of 6*10^{-2} MeV, the mass attenuation coefficient of Cu is $\mu / \rho = 1.593\ cm^2 / g$. Therefore, the result reported in this work has a relative error of 4.58%.

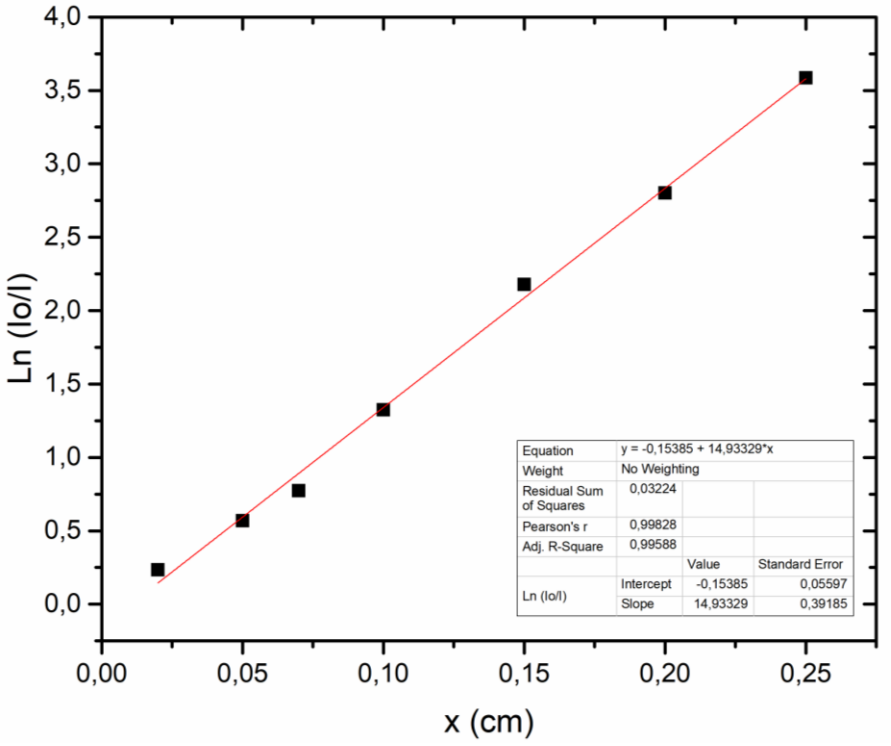

Figure 3 *Linear attenuation curve for Cu.*

4. Conclusions

The mass attenuation coefficients of Al and Cu were determined, which turned out to be $0.2913\ cm^2 / g$ and $1.666\ cm^2 / g$, respectively. Both with a relative error of less than 5% with respect to the values tabulated for the photon energy used.

References:

N. A. D. Silva. ***Laboratório Virtual de Física Moderna: Atenuação da Radiação Pela Matéria***. Cad. Bras. Ens. Fís., v. 29, n. 3: p. 1206-1231, dez. 2012.

Julián Orlando Páez López, Wilmar Rodríguez, D. Cano. ***Estudio de la atenuación en concreto para un haz de un acelerador a 6 MV***. Revista investigaciones y aplicaciones nucleares, ISSN-e 2711-1326, ISSN 2590-7468, n. 6: p. 81-89, 2022.

A. Sethi. ***X-Rays: Interaction with Matter***. Encyclopedia of Medical Devices and Instrumentation, Second Edition, edited by John G. Webster, John Wiley & Sons, 2006.

https://physics.nist.gov/PhysRefData/XrayMassCoef/ElemTab/z29.html